ISSN 1062-8738, Bulletin of the Russian Academy of Sciences: Physics, 2022, Vol. 86, No. 2, pp. 221–225. © Allerton Press, Inc., 2022.
Russian Text © The Author(s), 2022, published in Izvestiya Rossiiskoi Akademii Nauk, Seriya Fizicheskaya, 2022, Vol. 86, No. 2, pp. 287–292.

Synchronization in Interacting Networks of Hodgkin–Huxley Neurons

A. V. Andreev[a, *], V. A. Maksimenko[a], A. A. Badarin[a], V. V. Grubov[a, b], and A. E. Hramov[a]

[a] *Center for Neurotechnology and Machine Learning, Immanuel Kant Baltic Federal University, Kaliningrad, 236041 Russia*

[b] *Razumovsky State Medical University, Saratov, 410012 Russia*

**e-mail: andreevandrei1993@gmail.com*

Received October 1, 2021; revised October 11, 2021; accepted October 22, 2021

Abstract—A mathematical model of a "network of networks" is developed. The model consists of a small input network and four large subnetworks that interact with one another via inhibitory couplings. This model is an attempt to model processes that occur in real neural networks in similar processing of input information. It is shown the indices of synchronization of subnetworks periodically change in time. Depending on the strength of the connection, the indices of synchronization of neurons of different subnetworks can change in both phase and antiphase.

DOI: 10.3103/S1062873822020058

INTRODUCTION

Applying techniques from radiophysics, nonlinear dynamics, and network analysis to neurophysiological problems is a hallmark of modern science [1–4].

Different aspects of network theory are used in analyzing interaction between regions of the brain during cognitive activity [5, 6], based on experimental data (e.g., multi-channel records of electric and magnetic activity) [7–14] and numerical modeling of the interaction between individual neurons and groups of them by building networks with nonlinear elements [15–20]. The Hodgkin–Huxley [21], FitzHugh–Nagumo [22, 23], and Hindmarsh–Rose [24] models are used for neurons, depending on the strength of connection between the subnetworks and the elements inside them. The most complete of these is the Hodgkin–Huxley model, which describes the initiation and propagation of action potentials in light of ionic currents in the membranes of neurons. The spiking activity generated by this model simulates the electric activity of a real neuron.

Applying complex networks theory to neuroscience is a promising way of analyzing the structural and functional connections of brain neurons. Collective neuron activity plays an important role in the functioning of the brain [25]. According to functional magnetic resonance (fMRI) studies, the network activity of the entire brain is generated through the interaction between several functional subnetworks when resting or performing a task [26]. Collective processes that occur as a result of functional interaction between remote populations of cortical neurons support cognitive abilities when performing difficult tasks. Our current understanding of neuronal communication emphasizes the vital role of phase coherence in functional interaction between distant neuron ensembles.

We have developed a "network of networks" model that consists of one small input neural network and four big neural networks. An external signal received by the input network is transformed into a series of spikes that are then transmitted to the four subnetworks, which interact with one another via an inhibitory coupling to process the signal. This model is an analog of the information processing system in human brain, where a small input network receives information and transmits it for subsequent processing. Depending on the complexity of the input information, it can activate varying numbers of neural networks. The visual system is one example of such work in the brain, where signals from the thalamus are transmitted to the visual cortex. We found the indices of synchronization in the subnetworks periodically oscillate over time. These oscillations display either cophased or antiphased synchronization, depending on the strength of the inhibitory coupling between the subnetworks.

MODEL

We used the Hodgkin–Huxley model of a neuron described by the equations [21]

$$C_{\mathrm{m}}\frac{dV}{dt} = -g_{\mathrm{Na}}m^3h\left(V - V_{\mathrm{Na}}\right) - g_{\mathrm{K}}n^4\left(V - V_{\mathrm{K}}\right) - g_{\mathrm{L}}\left(V - V_{\mathrm{L}}\right) + I^{\mathrm{ex}} + I^{\mathrm{syn}}, \quad (1)$$

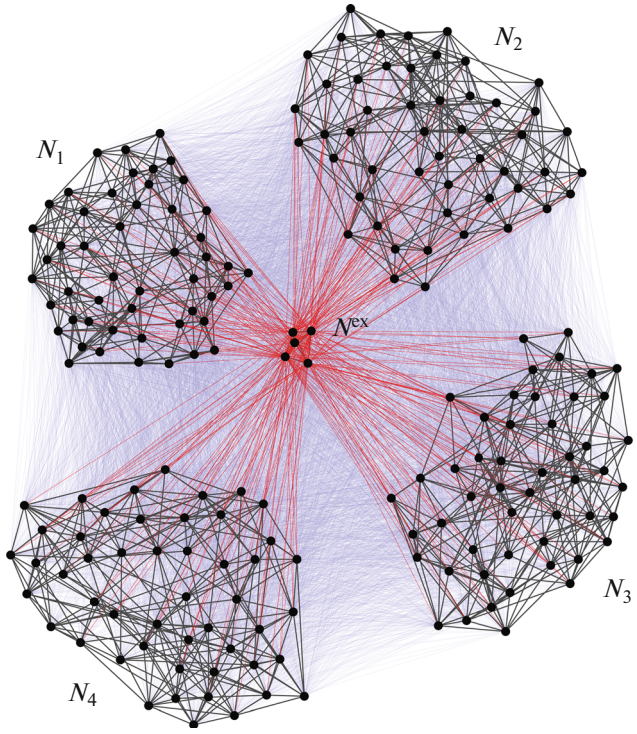

Fig. 1. Model of our "network of networks." The external signal with constant amplitude A is applied to the input network consisting of five neurons. Each neuron of the input network is unidirectionally connected with each of $N_1 = N_2 = N_3 = N_4 = 50$ neurons of the four subnetworks via excitatory synapses with coupling strength $g_c = 0.05$ and probability 30%. All subnetworks are bidirectionally interconnected via inhibitory synapses with coupling strength g_c^{ex} and probability 30%. The neurons in each network are connected with one another according to small-world topology with strength of connection g_c^{in}.

where $C_m = 1\ \frac{\mu F}{cm^3}$ is the membrane capacity per unit of area; I^{ex} is an external current; V is the membrane potential of the neuron in mV; $g_{Na} = 120\ \frac{mS}{cm^2}$, $g_K = 136\ \frac{mS}{cm^2}$, and $g_L = 0.3\ \frac{mS}{cm^2}$ indicate the maximum sodium, potassium, and leakage conductance when all ion channels are open; $V_{Na} = 50$ mV, $V_K = -77$ mV, and $V_L = -54.4$ mV are the reverse potentials for sodium channels, potassium channels, and leakage, respectively; m and h are variables of the activation and inactivation of sodium channel opening; n is the variable of activation for potassium channels; and n^4 and m^3h are the middle parts of opened potassium channels and sodium ions within the limits of the patch membrane. Depending on functions $\alpha_x(V)$ and $\beta_x(V)$, the dynamics of variables $x = m, n, h$ is specified as

$$\frac{dx}{dt} = \alpha_x(V)(1-x) - \beta_x(V)x, x = m, n, h, \qquad (2)$$

where I_i^{syn} is the shared synaptic current received by the ith neuron. We consider the connection via chemical synapses. The synaptic currents take the form [27]

$$I_i^{syn} = \sum_{j \in neight(i)} g_c e^{\frac{-(t-t_0^j)}{\tau_{syn}}} (E_{rev} - V_i), \qquad (3)$$

where alpha function $\alpha(t)$ describes the temporal evolution of synaptic conductance; g_c is the maximum conductance of synaptic channel; t_0^j is the time when a pre-synaptic jth neuron generates a spike; and $\tau_{syn} = 3$ ms.

The structure of the network is presented in Fig. 1. In our model, an external signal of constant amplitude $A = 9\ \mu A/cm^2$ corresponding to the mode of continuous spike generation is applied to the input network, which consists of five neurons interconnected with randomly selected strengths of connection in the range of 0–0.15 mS/cm^2. Each neuron of the input network is unidirectionally connected with each of $N_1 = N_2 = N_3 = N_4 = 50$ neurons of the four large subnetworks via excitatory synapses with coupling strength $g_c = 0.05$ mS/cm^2 and probability 30%. All the large subnetworks are bidirectionally interconnected via inhibitory couplings with strength g_c^{ex} and probability 30%. Inside each subnetwork, all neurons are interconnected via bidirectional excitatory synapses with strength g_c^{in}. Small-world topology, generated with the Watts–Strogatz model [28], was chosen for parameter value $\beta = 0.3$ and $K = 5$. We chose this network topology to model signal processing in the brain at low and at high levels (i.e., at the levels of individual neurons and neurons ensembles). The properties of small-world topology in real neuron ensembles determine the connections between neurons on the anatomical level [29, 30], allowing us to use this topology to model individual groups of neurons. The networks in this work are considered to be fairly close to one another, making it possible to interconnect all of them when a finite probability of establishing connections is introduced. A continuous stimulus received by the small input network is transformed into a series of spikes (amplitude-to-frequency transform) and transmitted to the large networks for the processing of the signal. A similar process occurs in the brain when perceiving visual information. The frequency of generating neuron ensembles involved in processing grows along with the flow of information. Neurons in each subnetwork are interconnected with strength of connection g_c^{in}.

RESULTS AND DISCUSSION

We analyzed the dynamics of "network of networks." An example of the typical temporal form of the complete neuron ensemble is given in Fig. 2a. Inside each subnetwork, all neurons generate spikes at nearly the same time because of the excitatory couplings between them. When averaged by all neurons of each subnetwork, the signals thus have series of individual concentrated spikes (Fig. 2b). One can see that under the effect of the inhibitory couplings, the four subnetworks split into two clusters. The first network is synchronized with the fourth; the second, with the third. Synchronized with each other, the networks generate spikes in equal time intervals, while the activity of networks from different clusters demonstrate antiphase dynamics. The two groups of subnetworks are thus in constant antiphase to each other. Since these subnetworks process the signal received from the small input network, we may conclude that the two groups of subnetworks split the input information between each other in order to work best, and the networks in each group must be synchronous for effective processing of the input signal.

To analyze the dynamics, we calculated the indices of synchronization between all neurons of each large subnetwork [31, 32]:

$$S = \sqrt{\frac{1}{T - t_0}\int_{t_0}^{T} \xi_n dt}, \qquad (4)$$

where t_0 is the period of transition; T is the total time; and ξ_n is the root-mean-square deviation, defined as

$$\xi_n = \frac{1}{N}\sum_{i=1}^{N}\left(x_n^{(i)}\right)^2 - \left(\frac{1}{N}\sum_{i=1}^{N} x_n^{(i)}\right)^2, \qquad (5)$$

where N is the number of elements in the network.

The resulting time series were then filtered in the 0.004–0.015 Hz range of frequencies to visualize slow changes. These indices can correlate with one another to varying degrees, depending on the coupling strength between the subnetworks and the elements inside them. To analyze these correlations, we calculated Pearson linear correlation coefficient r for each pair of subnetworks:

$$r = \frac{\int_{t_0}^{T}\left(S_1(t) - \bar{S}_1\right)\left(S_2(t) - \bar{S}_2\right)dt}{\sqrt{\int_{t_0}^{T}\left(S_1(t) - \bar{S}_1\right)^2\left(S_2(t) - \bar{S}_2\right)^2 dt}}, \qquad (6)$$

where S_1 and S_2 are the indices of synchronization of the first and second subnetworks; t_0 is the period of transition; T is the total time; and $r = 1$ and $r = -1$ denote fully positive and fully negative correlation, respectively.

We found that in the range of the considered coupling strengths, the first network displayed almost no correlation with the rest of the subnetworks at low values of internetwork connection, which fall to $r = -0.2$ upon an increase in inhibitory couplings (Fig. 3). The three other subnetworks act quite differently. With weak internetwork connections, the correlation between their indices of synchronization is close to 0, but it rises to 1.0 as this connection grows. We should note, that an increase in the strength of intranetwork connections improves the correlation between all networks.

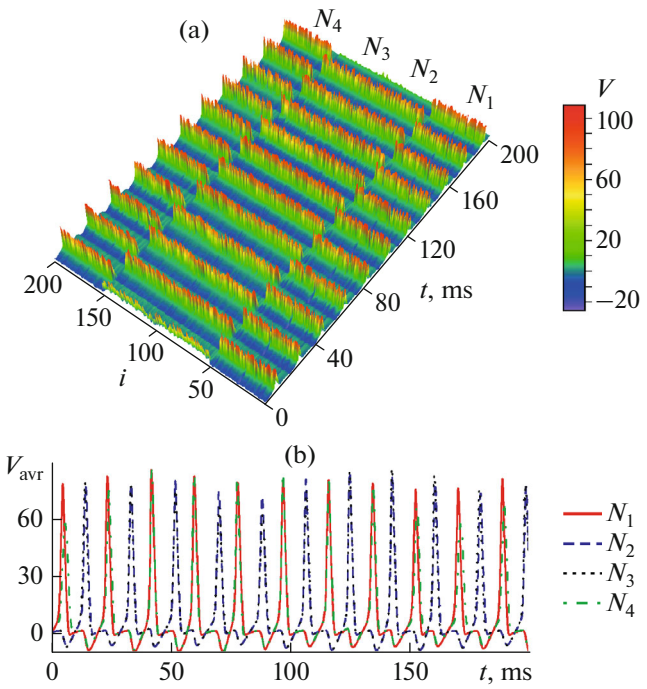

Fig. 2. (a) Spatiotemporal diagram of membrane potential V of neurons in the first N_1 ($i = 1, ..., 50$), second N_2 ($i = 51, ..., 100$), third N_3 ($i = 101, ..., 150$), and fourth N_4 ($i = 151, ..., 200$) network. (b) Time series of membrane potential, averaged over each subnetwork at $g_c^{ex} = 0.9$, $g_c^{in} = -0.03$.

CONCLUSIONS

A "network of networks" model has been developed that consists of a small input network and two large subnetworks. External signals received by the input network are transformed into a series of spikes that are then transmitted to two subnetworks with small-world topology that interact with each other via an inhibitory couplings to process the signal.

We analyzed the dynamics of the model network and found that the indices of synchronization in the subnetworks oscillate periodically over time, and low-frequency modulation arises. According to the literature, the low-frequency modulation of neuron spiking activity occurs due to rhythms of cortical activity (e.g.,

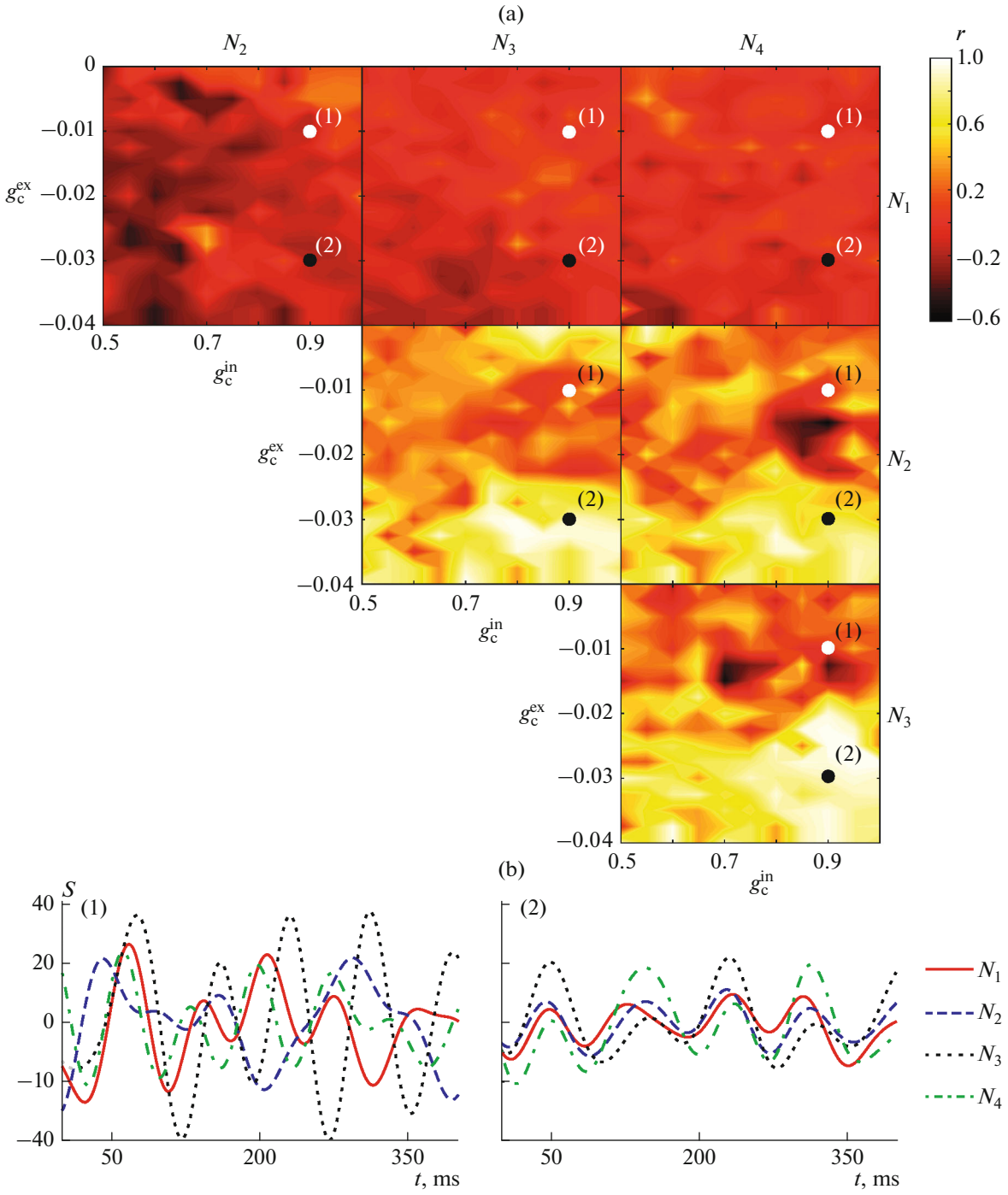

Fig. 3. (a) Two-parameter dependences of correlation r between indices of synchronization of the four subnetworks in the space of the coupling strengths between the subnetworks and elements inside them g_c^{in}. (b) Time dependences of indices of synchronization S for the four subnetworks, corresponding to points (1) $g_c^{ex} = 0.9$, $g_c^{in} = -0.01$ and (2) $g_c^{ex} = 0.9$, $g_c^{in} = -0.03$ in Fig. 3a.

theta, alpha, and beta) recorded noninvasively by EEGs. The indices of synchronization of these networks make cophased or antiphased oscillations when the strength of inhibitory connections between the networks is regulated. In the first case, a functional connection between these networks can be established; in the second, signals coming from one network to another will be blocked. We may assume

inhibitory couplings are possible regulators of cognitive resource redistribution among neuron ensembles in the brain. Our theoretical results indicate one possible mechanism of cognitive resource redistribution among neuron ensembles in the brain. According to our hypothesis, the brain dynamically redistributes the load between different neuron ensembles during prolonged activity, adjusting phase relations between their signals. At the same time, the activity of individual ensembles changes over time according to a periodic law, with alternating intervals of activation and recovery.

It was shown that maintaining a neural network in cophased or antiphased regimes of synchronization index oscillations requires keeping a balance between intra- and internetwork connections. The mechanism of joint information processing by separate groups of elements can be observed in both the work of different areas of the brain and the collective work of a group of people when solving one problem.

FUNDING

This work was supported by the RF Presidential Grant Council, project no. NSh-589.2022.1.2. V.V. Grubov thanks the Russian Foundation for Basic Research for their support as part of project no. 19-32-60033.

CONFLICT OF INTEREST

The authors declare that they have no conflicts of interest.

REFERENCES

1. Betzel, R.S., Gu, S., Medaglia, J.D., et al., *Sci. Rep.*, 2016, vol. 6, 30770.
2. Hermundstad, A.M., Bassett, D.S., Brown, K.S., et al., *Proc. Natl. Acad. Sci. U. S. A.*, 2013, vol. 110, p. 6169.
3. Hramov, A.E., Koronovskii, A.A., Makarov, V.A., et al., *Wavelets in Neuroscience*, Berlin: Springer, 2015.
4. Atasoy, S., Donnelly, I., and Pearson, J., *Nat. Commun.*, 2016, vol. 7, no. 1, p. 1.
5. Thomas, J.P. and Gauthier, I., *Nat. Rev. Neurosci.*, 2004, vol. 5, p. 291.
6. Haenschel, C., Vernon, D.J., Dwivedi, P., et al., *J. Neurosci.*, 2005, vol. 25.
7. Campbell, I.G., *Curr. Protoc. Neurosci.*, 2009, vol. 49, no. 1, p. 10.
8. Buzsaki, G., *Nat. Neurosci.*, 2004, vol. 7, no. 5, p. 446.
9. Badarin, A.A., Skazkina, V.V., and Grubov, V.V., *Proc. SPIE*, 2020, vol. 11459, 114590D.
10. Buzsaki, G. and Draguhn, A., *Science*, 2004, vol. 304, p. 1926.
11. Kurkin, S., et al., *Eur. Phys. J. Plus*, 2021, vol. 136, no. 5, p. 548.
12. Frolov, N., Maksimenko, V., and Hramov, A., *Chaos*, 2020, vol. 30, no. 12, 121108.
13. Maksimenko, V.A., Frolov, N.S., Hramov, A.E., et al., *Front. Behav. Neurosci.*, 2019, vol. 13, p. 220.
14. Frolov, N.S., Maksimenko, V.A., Hramova, M.V., et al., *Eur. Phys. J.: Spec. Top.*, 2019, vol. 228, no. 11, p. 2381.
15. Valencia, M., Martinerie, J., Dupont, S., et al., *Phys. Rev. E*, 2008, vol. 77, no. 5, 050905.
16. Andreev, A.V., Maksimenko, V.A., Pisarchik, A.N., et al., *Chaos, Solitons Fractals*, 2021, vol. 146, 110812.
17. Klinshov, V., Shchapin, D., Yanchuk, S., and Nekorkin, V., *Phys. Rev. Lett.*, 2015, vol. 114, no. 17, 178103.
18. Andreev, A. and Maksimenko, V., *Cybern. Phys.*, 2019, vol. 8, no. 4, p. 199.
19. Klinshov, V.V., Teramae, J., Nekorkin, V.I., and Fukai, T., *PloS One,* 2014, vol. 9, no. 4, e94292.
20. Ponomarenko, V.I., Kulminskiy, D.D., Andreev, A.V., and Prokhorov, M.D., *Tech. Phys. Lett.*, 2021, vol. 47, no. 2, p. 162.
21. Hodgkin, A.L. and Huxley, A.F., *J. Physiol.*, 1952, vol. 117, no. 4, p. 500.
22. Fitz, H.R., *Biophys. J.*, 1961, vol. 1, no. 6, p. 445.
23. Nagumo, J., Arimoto, S., and Yoshizawa, S., *Proc. IRE*, 1962, vol. 50, no. 10, p. 2061.
24. Hindmarsh, J.L. and Rose, R.M., *Proc. R. Soc. London, Ser. B*, 1984, vol. 221, no. 1222, p. 87.
25. Bullmore, E. and Sporns, O., *Nat. Rev. Neurosci.*, 2009, vol. 10, no. 3, p. 186.
26. van den Heuvel, M.P. and Pol, H.E.H., *Eur. Neuropsychopharm.*, 2010, vol. 20, no. 8, p. 519.
27. White, J.A., Rubinstein, J.T., and Kay, A.R., *Trends Neurosci.*, 2000, vol. 23, no. 3, p. 131.
28. Watts, D.J. and Strogatz, S.H., *Nature*, 1998, vol. 393, no. 6684, p. 440.
29. Muldoon, S.F., Bridgeford, E.W., and Bassett, D.S., Sci. Rep., 2016, vol. 6, 22057.
30. Bassett, D.S. and Bullmore, E., *Neuroscience*, 2006, vol. 12, p. 512.
31. Wang, Q., Perc, M., Duan, Z., and Chen, G., *Phys. Rev. E*, 2009, vol. 80, no. 2, 026206.
32. Sausedo-Solorio, J.M. and Pisarchik, A.N., *Eur. Phys. J.: Spec. Top.*, 2017, vol. 226, no. 9, p. 1911.

Translated by A. Khaitin